Serveur Académique Lausannois SERVAL serval.unil.ch

Author Manuscript
Faculty of Biology and Medicine Publication

This paper has been peer-reviewed but dos not include the final publisher proof-corrections or journal pagination.

Published in final edited form as:

Title: (18)F-fluorodeoxyglucose positron emission tomography/computed tomography and magnetic resonance imaging in patients with liver metastases from uveal melanoma: results from a pilot study.
Authors: Orcurto V, Denys A, Voelter V, Schalenbourg A, Schnyder P, Zografos L, Leyvraz S, Delaloye AB, Prior JO
Journal: Melanoma research
Year: 2012 Feb
Volume: 22
Issue: 1
Pages: 63-9
DOI: 10.1097/CMR.0b013e32834d3dcb

In the absence of a copyright statement, users should assume that standard copyright protection applies, unless the article contains an explicit statement to the contrary. In case of doubt, contact the journal publisher to verify the copyright status of an article.

serval
serveur académique lausannois

UNIL | Université de Lausanne
Faculté de biologie et de médecine

Original research

FDG PET/CT and MR Imaging in Patients with Liver Metastases from Uveal Melanoma: Results from a Pilot Study

Victoria Orcurto, MD,[1] Alban Denys, MD,[2] Verena Voelter, MD,[3] Ann Schalenbourg, MD,[4] Pierre Schnyder, MD,[2] Leonidas Zografos, MD,[4] Serge Leyvraz, MD,[3] Angelika Bischof Delaloye, MD,[1] John O. Prior, PhD, MD[1]

From the Departments of [1]Nuclear Medicine, [2]Radiology and [3]Oncology Centre Hospitalier Universitaire Vaudois and University of Lausanne, Rue du Bugnon 46, CH-1011 Lausanne, Switzerland, [4]Jules-Gonin Eye Hospital, University of Lausanne, Av. de France 15, 1000 Lausanne 7, Switzerland

Running Title: FDG PET/CT and MRI in Liver Metastases from Uveal Melanoma

Disclosure: This study had no financial support. J.O.P. was recipient of an Academic Research Award from the Leenaards Foundation (Lausanne, Switzerland).

Word counts: 2,630 words

Corresponding author: J. O. Prior, CHUV University Hospital, Rue du Bugnon 46, CH-1011 Lausanne, Switzerland,
Phone +41 21 314 4348, FAX+41 21 314 4349,
john.prior@chuv.ch

ABSTRACT (245 words)

Purpose: ^{18}F-fluorodeoxyglucose (FDG) PET/CT and MRI are used for detecting liver metastases from uveal melanoma. The introduction of new treatment options in clinical trials might benefit from early response assessment. Here, we determined the value of FDG PET/CT with respect to MRI at diagnosis and its potential for monitoring therapy.

Material and Methods: Ten patients with biopsy-proven liver metastases of uveal melanoma enrolled in a randomized phase III trial (NCT00110123) underwent both FDG-PET coupled with unenhanced CT and Gadolinium-DTPA-enhanced liver MRI within 4 weeks. FDG PET and MRI were evaluated blindly and then compared using the ratio of lesion to normal liver parenchyma PET-derived standardized uptake value (SUV). The influence of lesion size and response to chemotherapy were studied.

Results: Overall, 108 liver lesions were seen: 34 (31%) on both modalities (1–18 lesions/patient), 4 (4%) by PET/CT only and 70 (65%) by MRI only. SUV correlated with MRI lesion size (r=0.81, P<0.0001). PET/CT detected 26/33 (79%) MRI lesions ≥1.2cm, while it detected only 8/71 (11%) lesions <1.2-cm (P<0.0001). MRI lesions without PET correspondence were small (0.6±0.2cm vs. 2.1±1.1cm, P<0.0001). During follow-up (6 patients, 30 lesions), the ratio lesion-to-normal-liver SUV diminished in size-stable lesions (1.90±0.64 to 1.46±0.50, P<0.0001), while it increased in enlarging lesions (1.56±0.40 to 1.99±0.56, P=0.032).

Conclusion: MRI outweighs PET/CT for detecting small liver metastases. However, PET/CT detected at least one liver metastasis per patient and changes in FDG uptake not related to size change, suggesting a role in assessing early therapy response.

Keywords: Uveal Melanoma; PET/CT; FDG; MRI; Liver Metastasis.

INTRODUCTION

Uveal melanoma is the most common primary intraocular malignancy in Caucasians, representing 70 % of all ocular tumors [1]. Median age at presentation is about 60 years and reported annual incidence ranges from 5.3–10.9 cases per million in the USA and 2–8 cases per million in Europe [2, 3]. Due to the lack of lymphatics in the eye, metastatic spread of uveal melanoma is exclusively hematogenous, predominantly to the liver (≥95% of metastatic patients) [4]. Around 1% of patients have demonstrable liver metastases at presentation, and up to 50% will ultimately develop hepatic metastases within 10-15 years, suggesting the presence of subclinical disease at the time of initial diagnosis [1]. The mechanisms for this liver tropism is not yet understood [4]. Other less common sites of metastasis are lungs, bones, skin, lymph nodes, pancreas, heart, spleen, adrenal glands, gastro-intestinal tract, kidneys, ovaries and thyroid. Several clinical, histopathological and cytogenetic characteristics are associated with poor prognosis including chromosomal abnormalities, the most important of which are monosomy 3, isochromosome 6p, trisomy 8, and isochromosome 8q [5].

Currently, there are no effective treatments to prevent, delay or treat liver metastases of uveal melanoma and median survival after diagnosis of liver metastasis is 2–7 months in historical series [6]. Several regional therapies are clinically used or under investigation in clinical trials to control liver progression, such as hepatic arterial chemotherapy, chemoembolization [6], radioembolization [7], thermoablation [8] or targeted therapies showing potential benefit on overall survival or response rate, even without objective tumor response [4, 9]. For instance, using intra-arterial hepatic fotemustine chemotherapy, median survival of up to 15 months has been observed in association with a 36% response rate and 33% survival rate at 2 years [10].

Positron emission tomography (PET) with ^{18}F-fluorodeoxyglucose (FDG) is a sensitive and an accurate method for the detection of metastases from cutaneous melanoma. Of limited value for the diagnosis of ocular melanoma, it was found to be sensitive for the detection of hepatic and extra-hepatic metastases [11-14]. Servois and coworkers compared the performance of FDG-PET and MRI for staging liver metastasis and concluded that MRI was superior to FDG-PET [15], but the respective value of FDG PET and MRI imaging have not been fully assessed in intra-patient comparison for the diagnosis and monitoring of liver metastasis from uveal melanoma [12]. Tumor uptake of FDG is highly reproducible and decrease is known to occur before change in size [16]. Whether this remains true for liver metastases from uveal melanoma is not known.

Early diagnosis of liver metastasis may be important for therapeutic management [17]. Furthermore early response assessment may benefit the introduction of new treatment options as key oncogenic processes leading to uveal melanoma have been recently identified [18]. Our purpose was to determine the respective value of FDG PET and MRI imaging in patients with liver metastases of uveal melanoma.

METHODS

Patient Selection

From 2004 to 2008, 10 patients with known uveal melanoma and at least one histologically-proven liver metastasis were enrolled in a randomized phase III multicentric trial from the Uveal Melanoma Group of the European Organization for Research and Treatment of Cancer (EORTC) comparing the effect on overall survival of hepatic intra-

arterial to systemic intravenous administration of fotemustine in patients with liver metastases from uveal melanoma (EORTC-18021, NCT00110123). This trial was initiated after a phase II trial at our center showed evidence for improved survival after intra-arterial hepatic fotemustine chemotherapy [19]. Eligibility criteria were age ≥18 years, surgically incurable or unresectable disease and no extrahepatic metastases; exclusion criteria were previous chemo or radiotherapy, abnormal hematopoiesis, abnormal kidney or liver function, uncontrolled angina pectoris, myocardial infarction <6 months, intracranial hypertension, other severe cardiac disease, other malignancy <5 years. Patients not having recovered from prior major surgery or with performance status not WHO >2 were also excluded. The protocol was approved by the local ethics committee and the Swiss regulatory authorities, and patients signed informed consent forms before inclusion.

At our center, this protocol included an imaging study comparing MRI imaging and FDG PET that is presented here. Ten patients (6 women, 4 men; 20–74 years at diagnosis) were studied by MRI and PET/CT within 4 weeks (range 0–25 days). Of them, 6 patients were studied at baseline and 4 early during chemo-induction (after 3–4 cycles of fotemustine). During follow-up, a subgroup of 6 patients repeated both PET/CT and MRI imaging studies within 4 weeks after a variable time on therapy (7–28 weeks).

MRI

Abdominal MRI images were acquired on a 1.5T (n=5) and 3T (n=5) scanner (Symphony, Siemens Healthcare, Erlangen, Germany) with a maximum gradient strength of 40 mT/m using a 4-channel phased-array body coil with a 35×25-cm FOV.

Bandwidth was 1346 Hz. The liver protocol encompassed a breath-hold, T2-weighted transverse half-Fourier single-shot turbo spin echo sequence (HASTE, repetition time/echo time=1100ms/59ms, echo train length=256, matrix=256×148, slab thickness/gap=3mm/0.9mm), a T1-weighted transverse spoiled gradient-echo (GE) sequence (in-phase: 167/4.8, out-phase: 167/2.4, 256×134, 6/2, flip angle 70°), a respiratory-triggered T2-weighted transverse fat-suppressed fast spin echo sequence (6361.3/121, echo train length=23, 512×188, 6/1.8) and a breath-hold T1-weighted transverse fat-suppressed GE sequences (VIBE, 3.7/1.6, 256×192, 4/0.8, flip angle 12°, 1 NEX). The latter was performed before and after intravenous Gd-DTPA injection (arterial, portovenous, and equilibrium phases; 0.1mmol/kg Omniscan, GE Healthcare). Liver lesions were considered suspicious for metastases when presenting a short T1 pattern (high signal intensity) without injection, an arterial Gd-DPTA enhancement and a short T2 pattern (low signal intensity) as compared to adjacent normal liver; solitary lesions with short T1 pattern and a long T2 pattern were also considered as suspicious [20].

FDG PET/CT

Whole-body PET/CT (Discovery LS scanner, GE Medical System) was acquired 67±15 min after intravenous bolus injection of FDG (5 MBq/kg) using standard PET/CT acquisition protocols. Patients had been fasting for ≥6 hours and blood glucose at injection was <8.3mmol/L. Attenuation correction was performed using an unenhanced CT (140 keV, 80 mA, 0.8s per rotation, table speed of 15 mm/rotation, slice thickness 5mm). Liver lesions were considered suspicious for metastases when FDG uptake was focally increased compared to surrounding liver on at least 2 consecutive 5-mm slices.

Image Analysis

An experienced radiologist evaluated the MRI images and an experienced nuclear medicine specialist evaluated the PET images. Each reader was blinded to the results of the other modality. For MR, hepatic lesions were numbered, evaluated and their largest diameter measured. For each suspicious liver lesion, maximal standardized uptake values (SUV) corrected for body weight were obtained. To facilitate result comparison with other PET centers, we expressed the lesion SUV normalized to normal liver parenchyma SUV ("*lesion-to-liver SUV ratio"*) by dividing the lesion SUV by liver SUV averaged in a volume of ≥27 cm^3 in a region with uniform activity on PET distant from areas with abnormally increased or decreased FDG uptake. In a second reading, MRI and PET images were subsequently compared to each other to classify each lesion as being detected by both (MR+PET) or a single modality (MRI or PET). The intrinsically low resolution of PET scanners and the 3-D voxel sampling contribute to the "*partial volume effect"*, which significantly diminishes the apparent SUV in lesions smaller than twice the PET scanner resolution [21]. Therefore, referring to the known spatial resolution of our scanner of about 6 mm [22], a subgroup analysis was performed according to lesion size <1.2 and ≥1.2 cm diameter.

Statistical Analysis

Results are presented as mean ± standard deviation (SD), if not specified otherwise. Group comparisons were made using unpaired Student's *t*-tests for continuous variables and the χ^2-test for categorical variables. Lesion changes from baseline to follow-up used paired Student's *t*-test, and associations were sought using Pearson's correlations. Significance was considered for *P* values <0.05.

RESULTS

Patient Characteristics

Table 1 summarizes patient and tumor characteristics: no patient presented with a T1 tumor, 1 with a T2 (10%), 7 with a T3 (70%) and 2 with a T4 (20%) tumor, according to the TNM-AJCC (American Joint Cancer Committee) classification [23] and three patients already had liver metastasis at primary diagnosis (M1). The median interval between the primary diagnosis of uveal melanoma and the detection of hepatic metastasis was 3.0 years (range: 0–10 years). No significant correlation was found between SUV on one hand and the total number of lesions, tumor height, largest basal diameter or TNM-AJCC classification on the other hand (all $P>0.44$).

Lesion Detection According Imaging Modality

Overall, 108 suspicious liver lesions were seen by MRI or PET (Table 2). Of these lesions, 34 (31%) were seen on both PET and MRI imaging, 4 (4%) only on PET and 70 (65%) only on MRI imaging among which 41 were seen in one patient (Figure 1 and Figure 2). On a per patient basis, at least one liver metastasis (range 1–18) was detected with PET in all patients.

Influence of Lesion Size

As expected, MRI more often detected small-sized lesions, while most lesions ≥1.2 cm could be seen on both modalities. Twenty-six out of 33 (79%) lesions ≥1.2 cm on MRI imaging were visualized by PET, while this was the case for only 8 out of 71 (11%) lesions <1.2 cm ($P<0.0001$). Moreover, lesions <1.2 cm had significantly lower SUV than larger ≥1.2 cm lesions (3.1±0.5 vs. 4.7±1.8 g/mL, $P<0.0001$) (Figure 3).

FDG PET Standardized Uptake Value

For lesions detected by both modalities, there was a strong correlation between SUV (*SUV* [g/mL]= 2.9 + 1.06 · *MRI size* [cm], $r = 0.76$, $P<0.0001$), as well as between the lesion-to-liver SUV ratio ($r = 0.81$, $P<0.0001$) and MRI lesion size (Figure 4). Of note, there were 8 subcentimetric lesions detected by PET with SUV significantly increased above liver background (3.8±0.5g/mL vs. 3.0±0.4g/mL, $P<0.0001$) (Figure 4). PET lesions with no corresponding MRI lesion presented significantly elevated SUV as compared to liver background (4.0±0.5g/mL vs. 3.0±0.4g/mL, $P<0.0001$) (Figure 5). MRI lesions without corresponding PET lesion were significantly smaller (0.6±0.2cm vs. 2.1±1.1cm, $P<0.0001$) (Figure 6).

Lesion Monitoring During Chemotherapy

Median time between baseline and follow-up imaging was 2.6 months (range 1.5–6.5) in the group of 6 patients imaged twice (n=30 lesions in total). As any change in lesion size can influence the measured SUV, a subgroup analysis was performed for lesions detected on both MRI and PET/CT according to change in lesion size (no significant change in size vs. increase in MR-measured largest lesion diameter). The mean SUV of liver did not change significantly from baseline to follow-up (2.93±0.46 vs. 2.81±0.25, $P=0.7$). In 5 patients, lesion size (26 lesions) did not change significantly, while 1 patient (4 lesions) progressed rapidly after 3.9 months, as illustrated in Figure 7. In stable lesions ($n=26$), lesion-to-liver SUV ratio significantly decreased (from 1.90±0.64 to 1.46±0.50, $P<0.0001$), while in growing lesions ($n=4$) lesion-to-liver SUV ratio increased (1.56±0.40 to 1.99±0.56, $P=0.032$).

DISCUSSION

Our study on 10 patients with hepatic metastases from uveal melanoma, totaling over 100 liver lesions observed on MRI and PET, only 31% of the secondary lesions were seen on both modalities whereas most lesions inferior to 1 cm were missed on FDG-PET. Our data therefore confirm the findings of Servois [15], showing that MRI outweighs PET/CT performance for detecting small-sized liver metastases. In consequence, MRI appears to be the preferred method for evaluating number and topography of liver metastases potentially treatable by local therapy such as surgery, radiofrequency ablation, chemo- or radioembolization. The partial volume effect and artifacts from respiratory movements during acquisition prevented detection of most small sized metastases. Nevertheless, a few infracentimetric lesions (11%) expressed increased FDG uptake. When considering larger sizes (≥1.2 cm), 79% of the lesions were visualized by both modalities. On a per-patient basis, FDG-PET proved to be a sensitive investigation, as it detected the presence of at least one liver metastasis in every patient of our population. This allowed observing changes in the metabolic activity of lesions between baseline and follow-up examinations, even in the absence of a change in lesion size on MRI.

Our study compared MRI imaging to FDG PET in the same patient. Francken et al. evaluated the detectability of liver metastasis by PET in a cohort of 22 patients, which showed a high sensitivity (10/10), a moderate specificity (67%) and positive and negative predictive values of 88% and 100% respectively [13]. They concluded that FDG-PET was particularly useful in the detection of isolated, potentially resectable liver metastases. The present work does not confirm these initial results, as many more liver lesions were detected by MRI imaging alone (PET detection rate 33%) whereas only 4 lesions were shown by FDG-PET and not by MRI. These lesions were of limited

extension (<3 pixels or <1.2cm) and of unknown origin (no histopathological proof was available, as it was deemed not clinically necessary for patient management). Thus an artifact at PET or a false negative MRI cannot be excluded. MRI should therefore be considered the method of choice for detecting liver metastases of uveal melanoma and characterizing liver involvement potentially amenable to local therapy. Our findings are in line with recent results by Strobel et al. showing limited value of FDG PET in the detection of liver metastasis from uveal melanoma as compared to cutaneous melanoma, with a PET detection rate of only 41% (11/27 metastases) [24].

Importantly, serial PET was able to detect short-term changes in the metabolic activity of lesions despite the absence of size change. This has significant implications for the early assessment of therapy response and FDG PET assessment of metastases has been proposed both as a surrogate marker of treatment response and as a prognostic factor for overall survival [25]. Identifying responders and non-responders might improve clinical management in term of side effects and costs [26].

Baseline SUV was found to be proportional to MRI size, including lesions with dimensions well above those where the partial volume effect is no longer expected to play a role. In fact, larger SUV values reflect increased rate of glycolysis and have been strongly associated with increased tumor aggressiveness and poorer outcome in a number of cancers such as lung cancer, esophageal cancer or thyroid carcinoma [25, 27]. Whether baseline SUV remains an independent prognostic marker in addition to the largest dimension of liver metastases needs to be verified in an outcome study following published guidelines [28].

Obviously, the small size and heterogeneity of our patient population does not allow to evaluate the effect of treatment response according to the administration route

or chemotherapeutic regimen, which is the aim of the multicentric EORTC-18021 study, but with over 100 lesions, comparisons between MRI and PET can be considered valid. Four patients had already started chemotherapy at first PET, which may diminish PET sensitivity. Another potential limitation is that the diagnosis of metastatic liver lesions was based on their characteristic MRI appearance, as it is obviously not possible to biopsy all liver lesions. Thus, false positive lesions at MRI cannot be excluded, but the combination of T1- and T2-weighting, and behavior after Gd-DTPA injection increase specificity. For a few patients, a dual-phase PET/CT was performed with a late phase taken after ≥90 min, which seemed to improve lesion detectability by increasing lesion SUV and lesion-to-liver SUV ratio (data not shown); delayed FDG-PET acquisition might therefore improve the detection of small metastases, as has been demonstrated for several other tumors as well as primary uveal melanomas [14]. Diffusion-weighted MRI was not performed in this study, but might be valuable in assessing response to therapy, if preliminary results showing treatment related changes in the apparent diffusion coefficient are confirmed [29]. Finally, our pilot study was not designed to determine the predictive value of PET or MRI for therapy response.

CONCLUSION:

In this pilot study, MRI outweighs FDG PET performance for detecting small-sized liver metastases and is therefore the preferred method for diagnosing the number and the topography of liver metastases. However, PET/CT showed decreased FDG uptake in absence of MRI change under chemotherapy and increased FDG uptake in lesions increasing in size at follow-up suggesting a possible role for monitoring treatment re-

sponse. This underlines the need of determining the value of FDG-PET/CT in predicting long-term response to therapy in patients with liver metastases from uveal melanoma in a prospective study.

ACKNOWLEDGMENT

This study had no financial support. J.O.P. was recipient of an Academic Research Award from the Leenaards Foundation (Lausanne, Switzerland).

CONFLICT OF INTEREST STATEMENT

None of the authors have a conflict of interest.

REFERENCES

1. Mudhar HS, Parsons MA, Sisley K, Rundle P, Singh A, Rennie IG. A critical appraisal of the prognostic and predictive factors for uveal malignant melanoma. *Histopathology* 2004; **45**:1-12.

2. Singh AD, Topham A. Incidence of uveal melanoma in the United States: 1973-1997. *Ophthalmology* 2003; **110**:956-961.

3. Virgili G, Gatta G, Ciccolallo L, Capocaccia R, Biggeri A, Crocetti E, *et al.* Incidence of uveal melanoma in Europe. *Ophthalmology* 2007; **114**:2309-2315.

4. Bakalian S, Marshall JC, Logan P, Faingold D, Maloney S, Di Cesare S, *et al.* Molecular pathways mediating liver metastasis in patients with uveal melanoma. *Clin Cancer Res* 2008; **14**:951-956.

5. Damato B, Dopierala J, Klaasen A, van Dijk M, Sibbring J, Coupland SE. Multiplex ligation-dependent probe amplification of uveal melanoma: correlation with metastatic death. *Invest Ophthalmol Vis Sci* 2009; **50**:3048-3055.

6. Feldman ED, Pingpank JF, Alexander HR, Jr. Regional treatment options for patients with ocular melanoma metastatic to the liver. *Ann Surg Oncol* 2004; **11**:290-297.

7. Kennedy AS, Nutting C, Jakobs T, Cianni R, Notarianni E, Ofer A, *et al.* A first report of radioembolization for hepatic metastases from ocular melanoma. *Cancer Invest* 2009; **27**:682-690.

8. Kuvshinoff B, Fong Y. Surgical therapy of liver metastases. *Semin Oncol* 2007; **34**:177-185.

9. Triozzi PL, Eng C, Singh AD. Targeted therapy for uveal melanoma. *Cancer Treat Rev* 2008; **34**:247-258.

10. Peters S, Voelter V, Zografos L, Pampallona S, Popescu R, Gillet M, *et al.* Intra-arterial hepatic fotemustine for the treatment of liver metastases from uveal melanoma: experience in 101 patients. *Ann Oncol* 2006; **17**:578-583.

11. Reddy S, Kurli M, Tena LB, Finger PT. PET/CT imaging: detection of choroidal melanoma. *Br J Ophthalmol* 2005; **89**:1265-1269.

12. Kurli M, Reddy S, Tena LB, Pavlick AC, Finger PT. Whole body positron emission tomography/computed tomography staging of metastatic choroidal melanoma. *Am J Ophthalmol* 2005; **140**:193-199.

13. Francken AB, Fulham MJ, Millward MJ, Thompson JF. Detection of metastatic disease in patients with uveal melanoma using positron emission tomography. *Eur J Surg Oncol* 2006; **32**:780-784.

14. Beyer T, Pietrzyk U, Knoess C, Vollmar S, Wienhard K, Kracht L, *et al.* Multi-modality imaging of uveal melanomas using combined PET/CT, high-resolution PET and MR imaging. *Nuklearmedizin* 2008; **47**:73-79.

15. Servois V, Mariani P, Malhaire C, Petras S, Piperno-Neumann S, Plancher C, *et al.* Preoperative staging of liver metastases from uveal melanoma by magnetic resonance imaging (MRI) and fluorodeoxyglucose-positron emission tomography (FDG-PET). *Eur J Surg Oncol* 2010; **36**:189-194.

16. Weber WA, Ziegler SI, Thodtmann R, Hanauske AR, Schwaiger M. Reproducibility of metabolic measurements in malignant tumors using FDG PET. *J Nucl Med* 1999; **40**:1771-1777.

17. Aoyama T, Mastrangelo MJ, Berd D, Nathan FE, Shields CL, Shields JA, *et al.* Protracted survival after resection of metastatic uveal melanoma. *Cancer* 2000; **89**:1561-1568.

18. Van Raamsdonk CD, Griewank KG, Crosby MB, Garrido MC, Vemula S, Wiesner T, *et al.* Mutations in GNA11 in uveal melanoma. *N Engl J Med* 2010; **363**:2191-2199.

19. Leyvraz S, Spataro V, Bauer J, Pampallona S, Salmon R, Dorval T, *et al.* Treatment of ocular melanoma metastatic to the liver by hepatic arterial chemotherapy. *J Clin Oncol* 1997; **15**:2589-2595.

20. Maeda T, Tateishi U, Suzuki S, Arai Y, Kim EE, Sugimura K. Magnetic resonance screening trial for hepatic metastasis in patients with locally controlled choroidal melanoma. *Jpn J Clin Oncol* 2007; **37**:282-286.

21. Soret M, Bacharach SL, Buvat I. Partial-volume effect in PET tumor imaging. *J Nucl Med* 2007; **48**:932-945.

22. Bolard G, Prior JO, Modolo L, Delaloye AB, Kosinski M, Wastiel C, *et al.* Performance comparison of two commercial BGO-based PET/CT scanners using NEMA NU 2-2001. *Med Phys* 2007; **34**:2708-2717.

23. American Joint Committee on Cancer. Malignant melanoma of the uvea. *AJCC Cancer Staging Manual*. 6th edn. New York, NY: Springer 2002: 365-370.

24. Strobel K, Bode B, Dummer R, Veit-Haibach P, Fischer D, Imhof L, *et al.* Limited value of ¹⁸F-FDG PET/CT and S-100B tumour marker in the detection of liver metastases from uveal melanoma compared to liver metastases from cutaneous melanoma. *Eur J Nucl Med Mol Imaging* 2009; **36**:1774-1782.

25. Larson SM, Schwartz LH. 18F-FDG PET as a candidate for "qualified biomarker": functional assessment of treatment response in oncology. *J Nucl Med* 2006; **47**:901-903.

26. Prior JO, Montemurro M, Orcurto MV, Michielin O, Luthi F, Benhattar J, *et al.* Early prediction of response to sunitinib after imatinib failure by 18F-fluorodeoxyglucose positron emission tomography in patients with gastrointestinal stromal tumor. *J Clin Oncol* 2009; **27**:439-445.

27. Downey RJ, Akhurst T, Gonen M, Vincent A, Bains MS, Larson S, *et al.* Preoperative F-18 fluorodeoxyglucose-positron emission tomography maximal standardized uptake value predicts survival after lung cancer resection. *J Clin Oncol* 2004; **22**:3255-3260.

28. Shankar LK, Hoffman JM, Bacharach S, Graham MM, Karp J, Lammertsma AA, *et al.* Consensus recommendations for the use of 18F-FDG PET as an indicator of therapeutic response in patients in National Cancer Institute Trials. *J Nucl Med* 2006; **47**:1059-1066.

29. Buijs M, Vossen JA, Hong K, Georgiades CS, Geschwind JF, Kamel IR. Chemoembolization of hepatic metastases from ocular melanoma: assessment of response with contrast-enhanced and diffusion-weighted MRI. *AJR Am J Roentgenol* 2008; **191**:285-289.

TABLES

Table 1. Patients and tumors characteristics

Patient #	Gender	Age* (years)	Eye side	Tumor size† (mm)		TNM-AJCC‡ (Stage)	Primary tumor therapy
				Height	Largest basal diameter		
1	Man	73	Right	2.9	13.1	T4N0M1 (IV)	Proton therapy
2	Woman	69	Left	3.1	14.2	T2N0M0 (II)	Proton therapy
3	Woman	30	Left	5.8	16.3	T3N0M0 (III)	Proton therapy
4	Man	39	Left	5.8	23.5	T3N0M0 (III)	Proton therapy
5	Woman	20	Left	6.8	15.6	T3N0M0 (III)	Proton therapy
6	Man	74	Right	7.0	7.0	T3N0M0 (III)	Enucleation
7	Man	56	Left	9.0	19.0	T3N0M0 (III)	Proton therapy
8	Woman	72	Right	11.4	19.1	T3N0M1 (IV)	Proton therapy
9	Woman	57	Right	12.7	23.3	T3N0M1 (IV)	Proton therapy
10	Woman	71	Left	16.0	15.0	T4N0M0 (III)	Enucleation

*At diagnosis of primary tumor.

†Tumor size of tumors treated by proton therapy cannot be compared to tumor size of enucleation, as the height and largest basal diameter were measured by ultrasound and preoperative transillumination respectively in the former and derived from the histo-pathology report in the latter.

‡AJCC = American Joint Cancer Committee Classification.

Table 2. PET and MRI imaging findings.

Patient	Number of MRI lesions	Number of PET lesions	Number of lesions seen both on PET & MRI (%)	Number of small-sized* lesions (mean [range], cm)
1	2	1	1 (50%)	2 (0.9 [0.8–1.0])
2	4	3†	2 (50%)	3 (0.8 [0.5–1.0])
3	2	2	2 (100%)	0 (–)
4	41	18	18 (44%)	20 (0.7 [0.3–1.1])
5	2	2†	1 (50%)	2 (0.9 [0.8–0.9])
6	26	4	4 (15%)	21 (0.5 [0.5–1.1])
7	3	3	3 (100%)	2 (0.8 [0.8–0.8])
8	4	2†	1 (25%)	3 (0.4 [0.4–0.4])
9	8	2†	1 (13%)	7 (0.5 [0.3–0.8])
10	12	1	1 (8%)	11 (0.5 [0.4–1.0])
Total	104	38	34 (33%)	71 ([0.3–1.1])

*Defined as size < 1.2 cm, which corresponds to twice the PET/CT spatial resolution [22].

†One PET lesion not visible on MRI.

FIGURE CAPTIONS

Figure 1. Lesion detectability according to imaging modality and lesion size. The vast majority of small lesions <1.2 cm, were only visualized by MRI imaging, while the larger lesions ≥1.2 cm were mostly visualized by both, MRI and PET. A few lesions were only detected on PET

Figure 2. FDG PET, PET/CT fusion, unenhanced CT and MRI transaxial images of two patients: (**A**) A 78-year-old man with several lesions detected on both PET and MRI (*arrows*) and several smaller lesions detected on MRI only (*arrowhead*) showing hyper-signal on T1-weighted fat-suppressed gradient-echo (TR 3.7ms, TE 1.6ms, flip angle 12°); (**B**) A 33-year-old woman with one 8-mm lesion detected on both PET and MRI (*arrow*) showing an hypersignal on unenhanced T1-weighted spoiled gradient-echo in-phase (TR 167ms, TE 4.8ms, flip angle 70°) and out-phase (TR 167ms, TE 2.4ms, flip angle 70°)

Figure 3. Boxplot of the lesion to liver standardized uptake value (SUV) ratio, which is significantly lower for smaller lesions (<1.2 cm) as compared to larger lesions (≥1.2 cm) ($P<0.0001$)

Figure 4. Plot of the standardized uptake value (SUV) of the lesion-to-liver SUV ratio vs. MRI lesion size for lesions visible on both modalities. There was a significant correlation between lesion-to-liver SUV ratio and lesion size, even above twice the PET/CT resolution ($y=0.79+0.44 \cdot x$, $r = 0.81$, $P<0.0001$). Note that 8 lesions smaller than twice the PET/CT resolution (1.2 cm, *dashed line*) were also detected on PET/CT

Figure 5. Boxplot of the ratio of lesion standardized uptake value (SUV) to liver parenchyma SUV according to visualization by MRI+PET or PET alone. The lesion-to-liver SUV ratio of lesions visible by both modalities (MRI+PET) was significantly higher than unity ($P<0.0001$)

Figure 6. Boxplot of the lesion size according to visualization by MRI+PET or MRI alone. The diameter of lesions visible by both modalities (MRI+PET) was significantly larger than lesions visible only by MRI ($P<0.0001$)

Figure 7. Variation in lesion-to-liver standardized uptake value (SUV) ratio between baseline (PET 1) and follow-up study (PET 2) according to change in lesion size as measured by MRI (no change vs. increase in size) for patients with lesions visible on both FDG-PET and MRI at baseline (6 patients, 30 lesions in total)

Figure 1

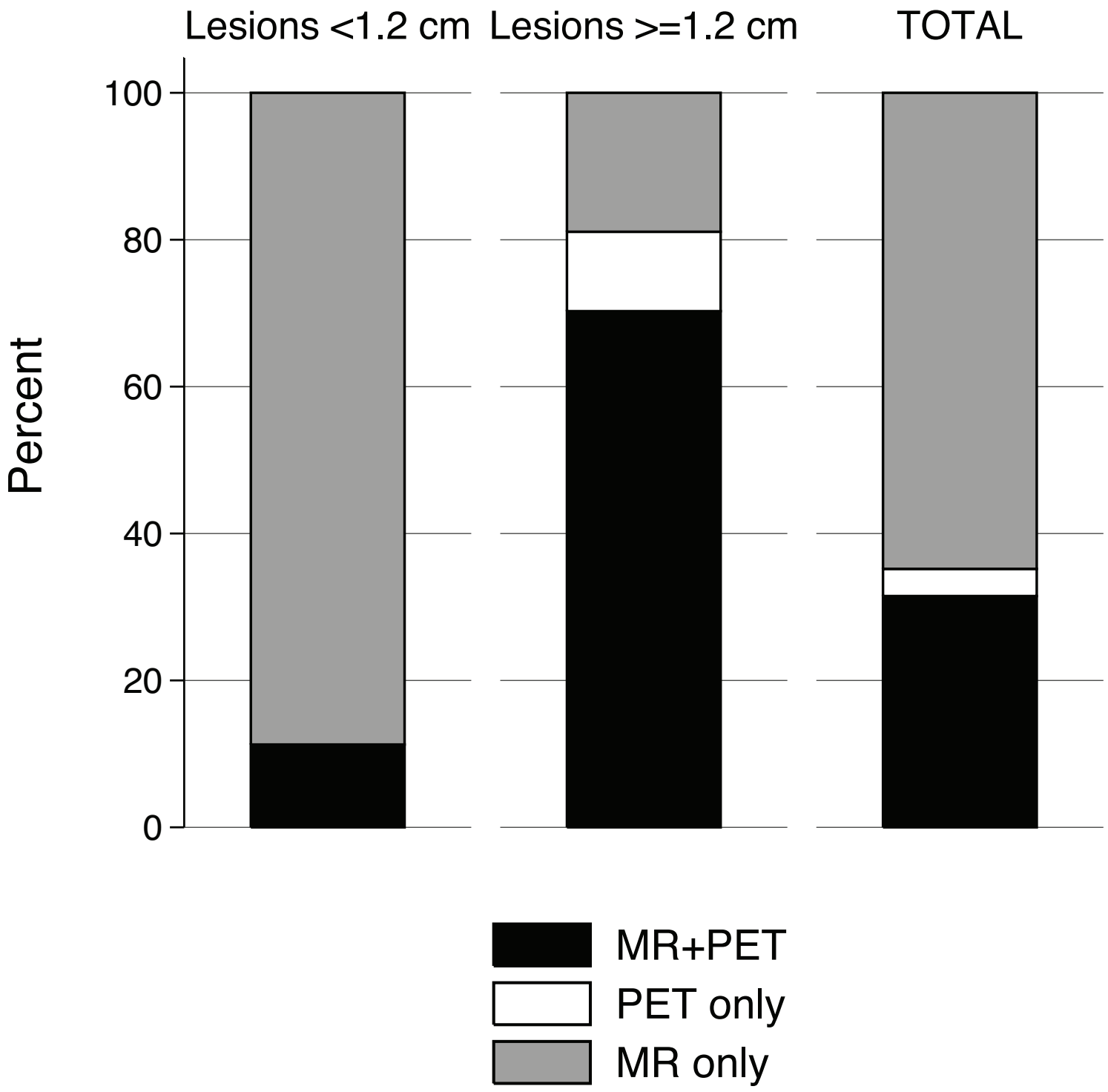
Lesions <1.2 cm
Lesions >=1.2 cm
TOTAL
Percent
100
80
60
40
20
0
MR+PET
PET only
MR only

Figure 2

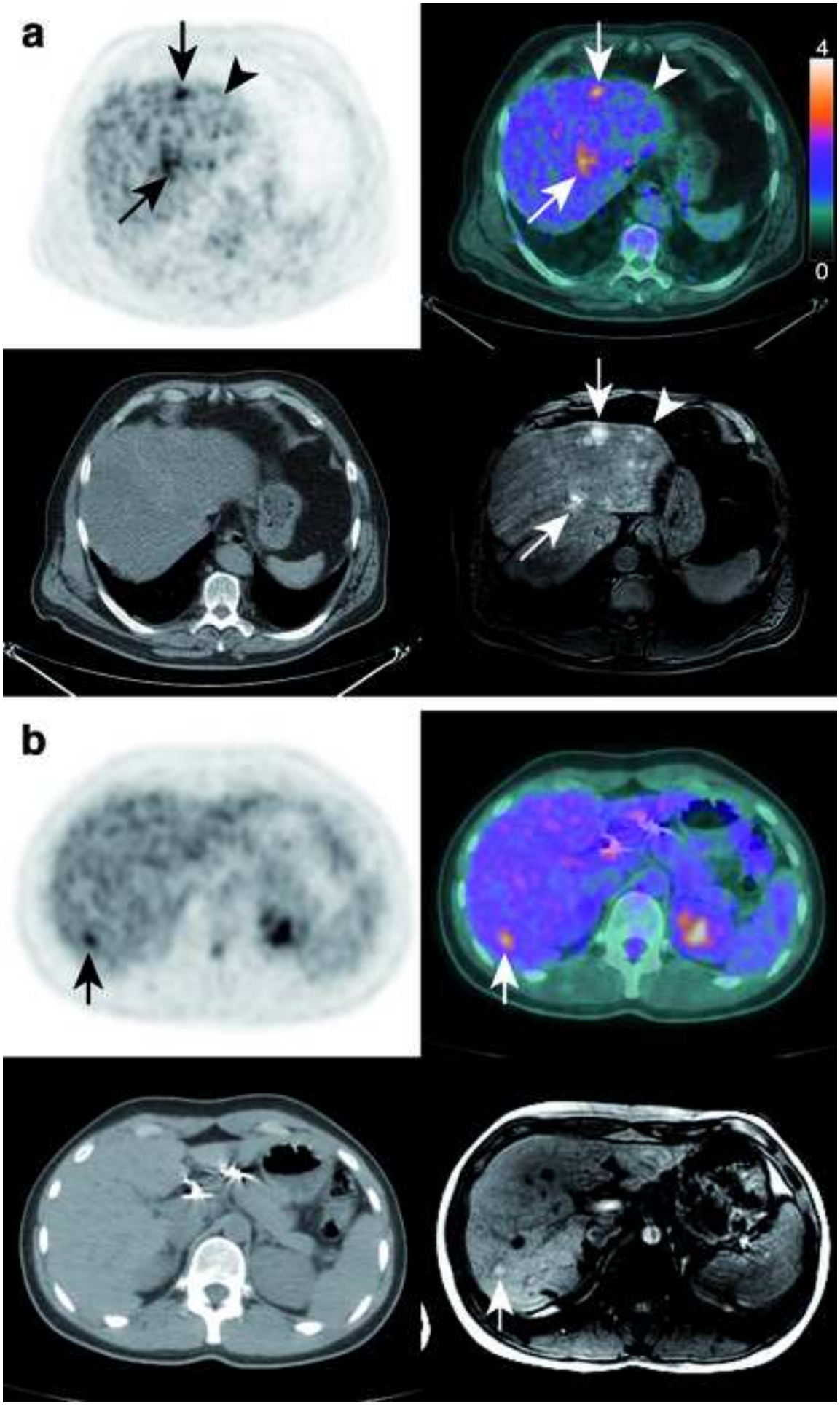

Figure 3

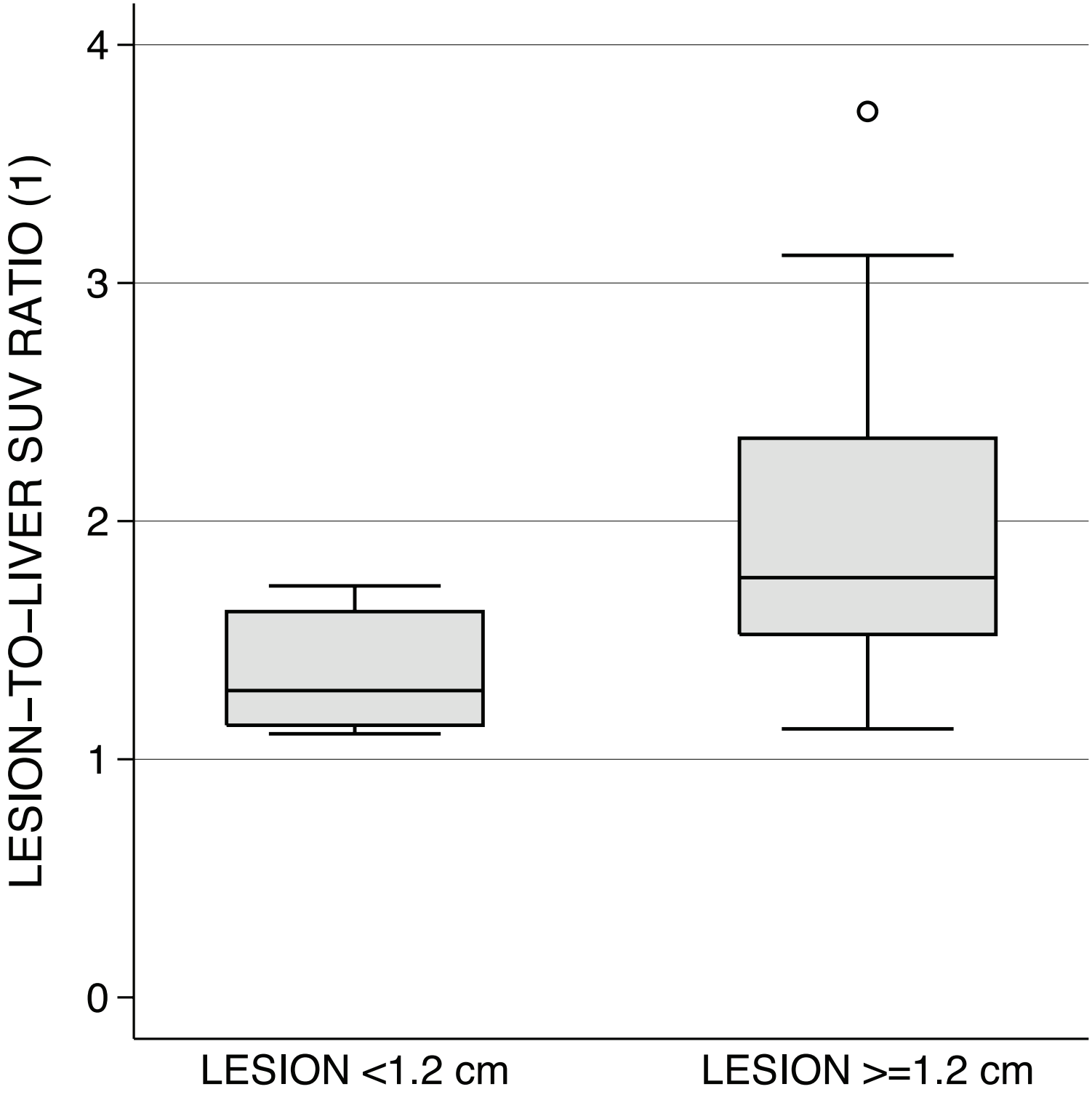

Figure 4

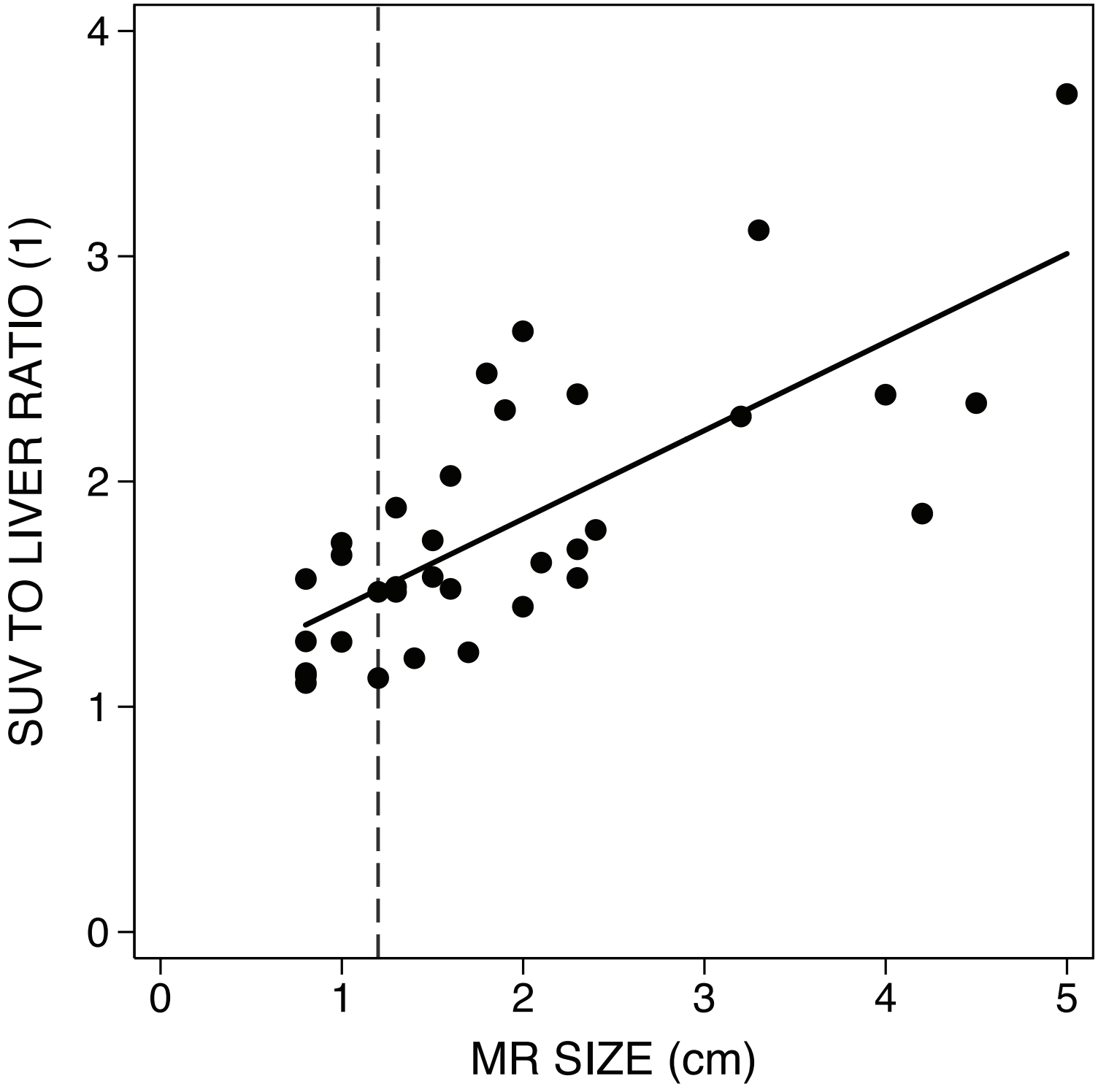

Figure 5

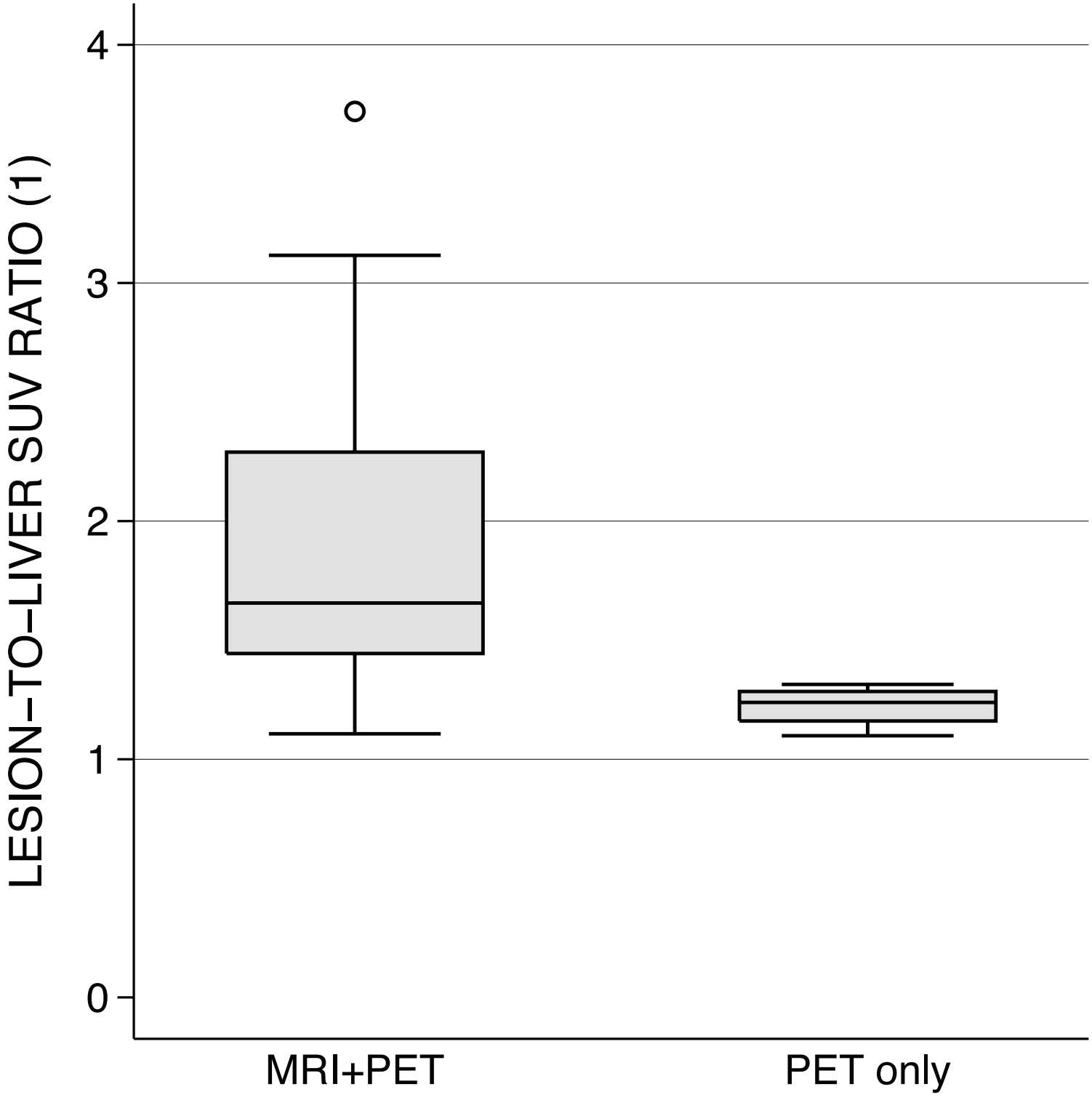

Figure 6

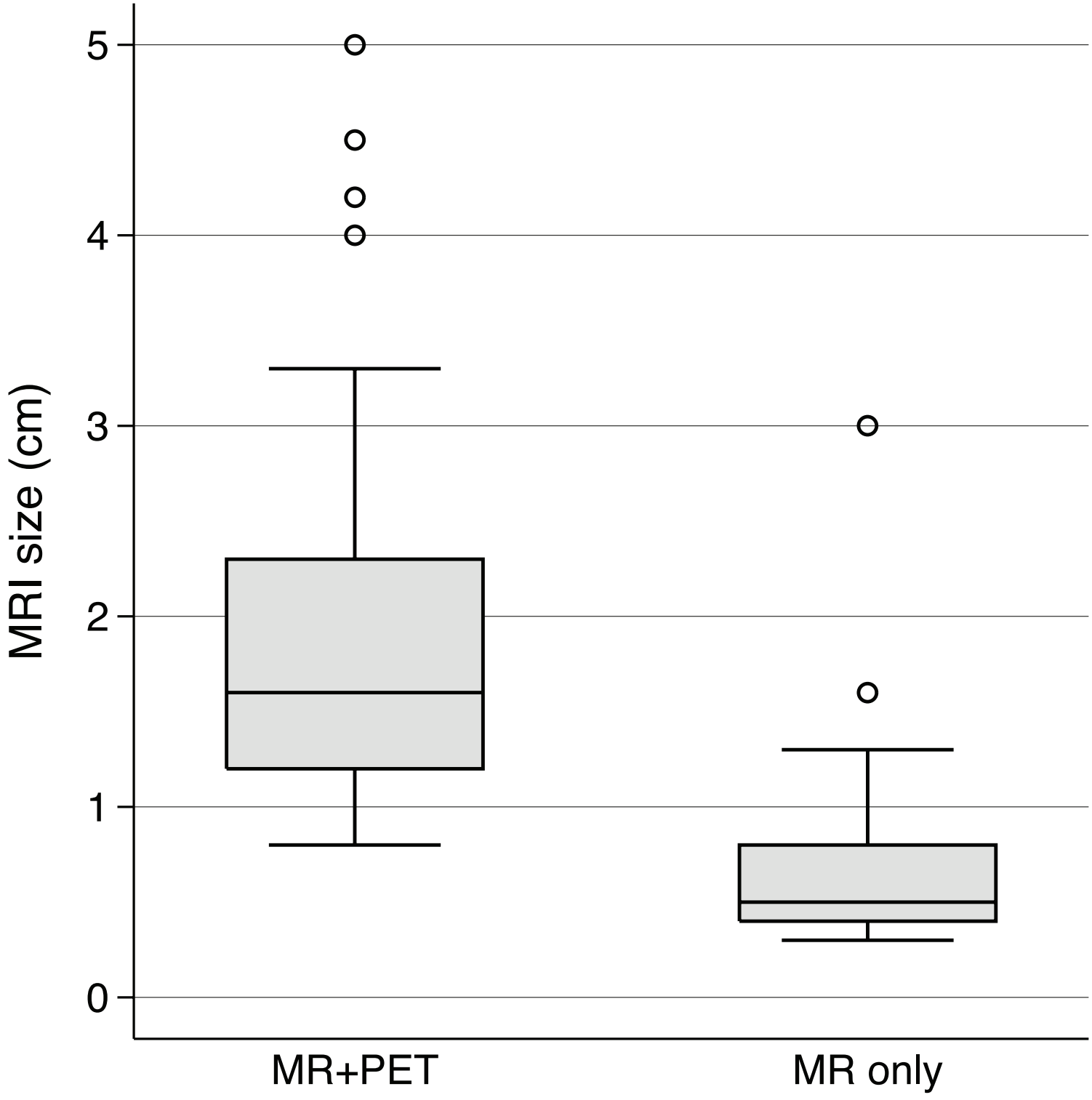

Figure 7

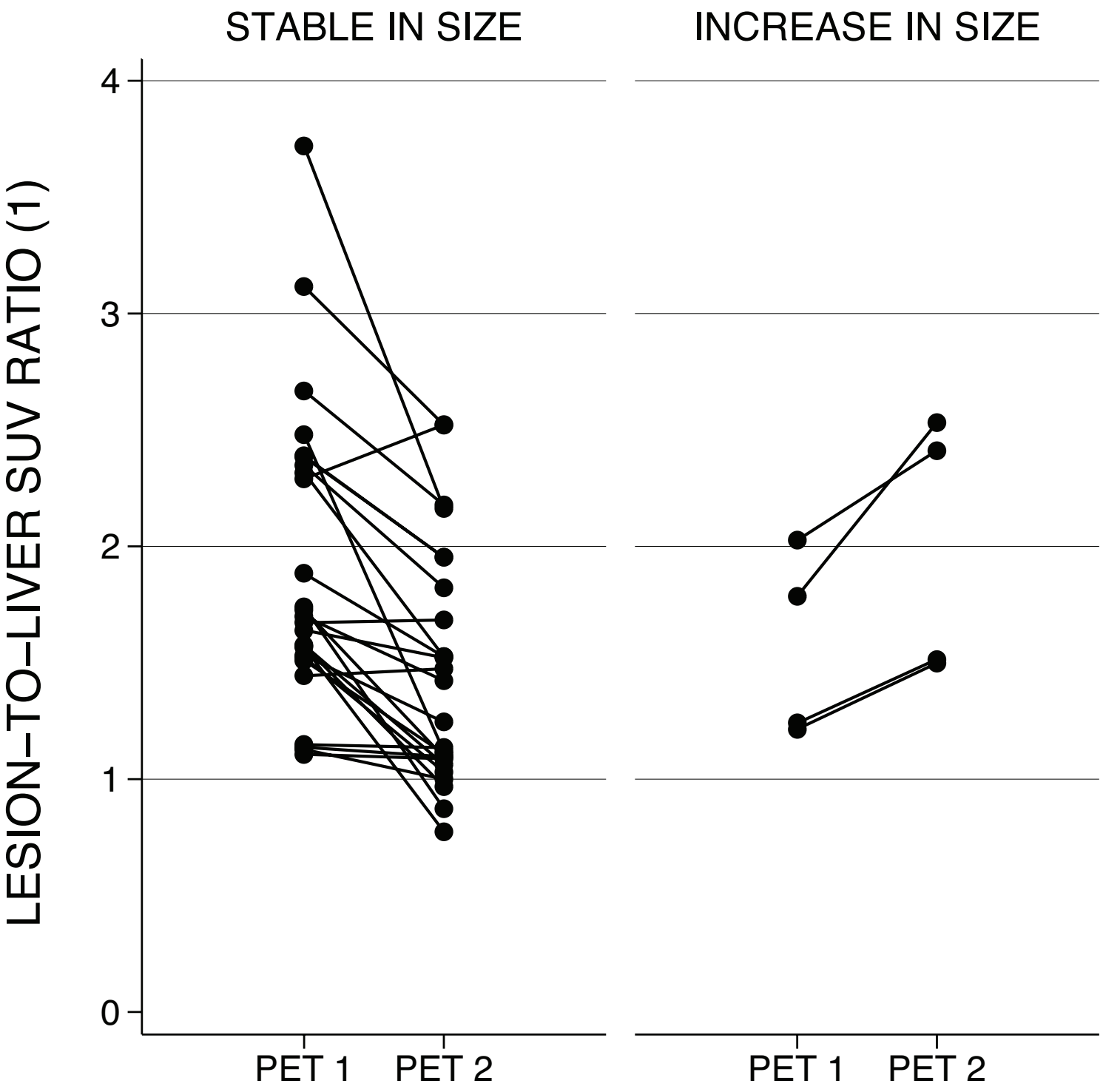
STABLE IN SIZE
INCREASE IN SIZE
LESION–TO–LIVER SUV RATIO (1)
4
3
2
1
0
PET 1
PET 2
PET 1
PET 2